Supporting Information

Tasinkevych et al. 10.1073/pnas.1405928111

SI Text

Details of Numerical Approach

Based on the Landau–de Gennes free energy (Eq. **1** in *Materials and Methods* of the main text) we find that the isotropic–nematic coexistence takes place at the value of reduced temperature $\tau \equiv 24a(T)c/b^2 = 1$ and that the degree of orientational order in the nematic phase is given by

$$Q_b = \frac{b}{8c}\left(1 + \sqrt{1 - \frac{8\tau}{9}}\right). \qquad \textbf{[S1]}$$

We assume $a(T) = a_0(T - T^*)$, where a_0 is a phenomenological material-dependent parameter; T^* is the supercoiling temperature of the isotropic phase. We use $a_0 = 0.044 \times 10^6$ J/m^3, $b = 0.816 \times 10^6$ J/m^3, $c = 0.45 \times 10^6$ J/m^3, $L_1 = 6 \times 10^{-12}$ J/m, and $L_2 = 12 \times 10^{-12}$ J/m [typical values for pentylcyanobiphenyl (5CB) (1) $T^* = 307$ K]. The size of topological defect cores is of the order of the bulk correlation length $\xi = 2(2c(3L_1 + 2L_2))^{1/2}/b \simeq 15$ nm at the isotropic–nematic transition (2).

In Cartesian coordinates $g = 1$ surface is described by an implicit equation $S_1(x,y,z) = 0$, with

$$S_1(x,y,z) \equiv \left(R - \sqrt{x^2 + y^2}\right)^{\alpha} + z^{\alpha} - r^{\alpha}, \qquad \textbf{[S2]}$$

where R and r are the major and the minor torus radius, respectively, and the exponent $\alpha \geq 2$ determines the tube's cross-sectional shape. The $g > 1$ surfaces may be constructed as a union of g (properly placed on a plane) [**S2**] surfaces. For example, we define the $g = 2$ handlebody surface implicitly as $S_2(x,y,z) = 0$, where

$$S_2(x,y,z) = \begin{cases} \left(R - \sqrt{(x-R)^2 + y^2}\right)^{\alpha} + z^{\alpha} - r^{\alpha}, & x > 0 \\ \left(R - \sqrt{(x+R)^2 + y^2}\right)^{\alpha} + z^{\alpha} - r^{\alpha}, & x \leq 0. \end{cases} \qquad \textbf{[S3]}$$

$g > 2$ surfaces may be described in an analogous way. We use the Open Source Gmsh library (3) to triangulate $g = 1$ surface [**S2**], and the Open Source GNU Triangulated Surface (GTS) library (4) for triangulation of $g > 1$ surfaces [**S3**]. The volume discretization is performed with the Quality Tetrahedral Mesh Generator (5). Linear triangular and tetrahedral elements are used in 2D and 3D, respectively. Generalized Gaussian quadrature rules for multiple integrals (6) are used to evaluate integrals over elements. In particular, for tetrahedra a fully symmetric cubature rule with 11 points (7) is used, and integrations over triangles are done by using a fully symmetric quadrature rule with 7 points (8). The discretized Landau–de Gennes functional is then minimized using the INRIA's M1QN3 (9). More information on the numerical procedures may be found in ref. 10.

1. Kralj S, Žumer S, Allender DW (1991) Nematic-isotropic phase transition in a liquid-crystal droplet. *Phys Rev A* 43(6):2943–2952.
2. Chandrasekhar S (1992) *Liquid Crystals* (Cambridge Univ Press, Cambridge, UK), 2nd Ed.
3. Gmsh: A three-dimensional finite element mesh generator (2014) Available at geuz.org/gmsh/. Accessed 2012.
4. Gnu Triangulated Surface Library (2006) Available at gts.sourceforge.net. Accessed September 2006.
5. Si H (2011) Tetgen: A quality tetrahedral mesh generator and a 3D Delaunay triangulator. Available at wias-berlin.de/software/tetgen/. Accessed September 2006.
6. Cools R (2003) An encyclopaedia of cubature formulas. *J Complexity* 19:445–453. Available at nines.cs.kuleuven.be/ecf/. Accessed September 2006.
7. Keast P (1986) Moderate-degree tetrahedral quadrature formulas. *Comput Methods Appl Mech Eng* 55:339–348.
8. Stroud AH (1971) *Approximate Calculation of Multiple Integrals* (Prentice-Hall, Englewood Cliffs, NJ).
9. Gilbert JC, Lemaréchal C (1989) Some numerical experiments with variable storage quasi-Newton algorithms. *Math Program* 45:407–436. Available at who.rocq.inria.fr/Jean-Charles.Gilbert/modulopt/optimization-routines/m1qn3/m1qn3.html. Accessed January 2005.
10. Tasinkevych M, Silvestre NM, Telo da Gama MM (2012) Liquid crystal boojum-colloids. *New J Phys* 14:073030.

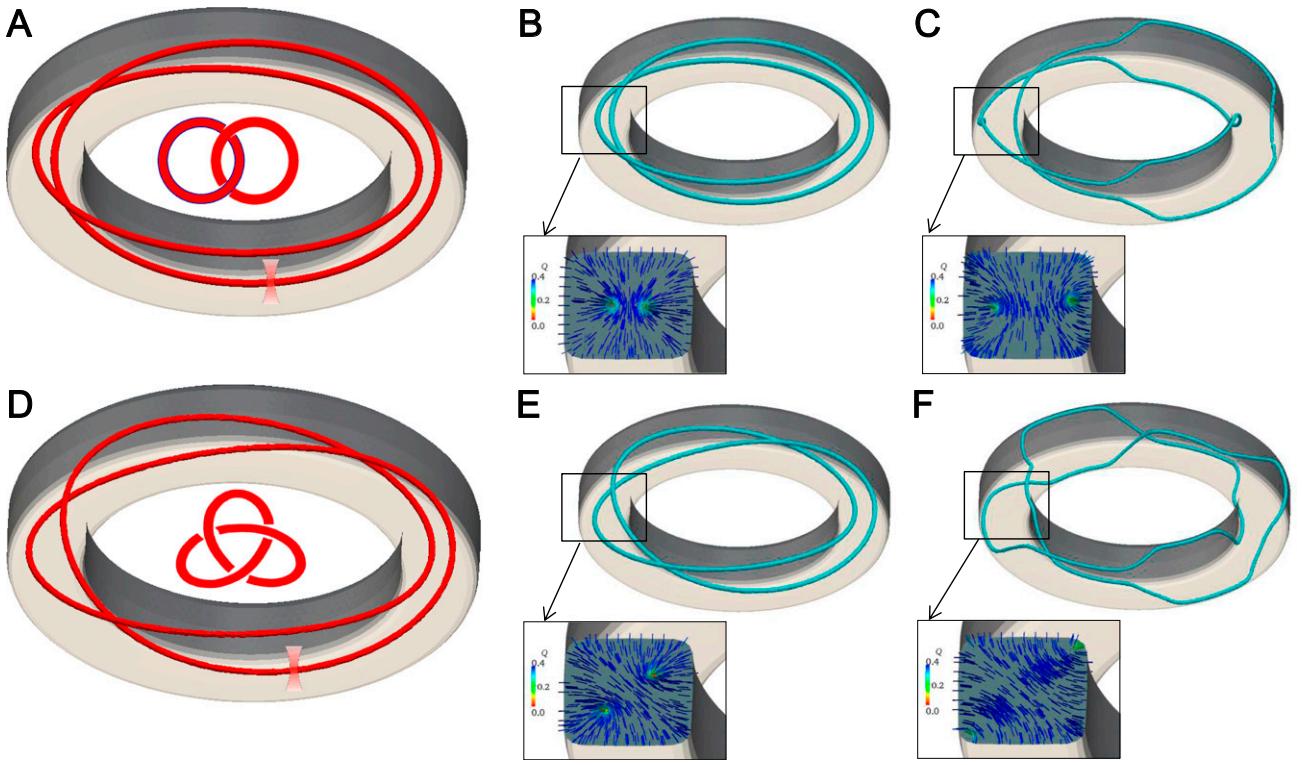

Fig. S1. Implementation of the laser-guided temperature quench which is used to generate a Hopf link (*A*–*C*) of two +1/2 disclination lines, and a trefoil knot (*D*–*F*) of an s = +1/2 disclination line. In *A* and *D*, the red surfaces enclose regions with temperature above the nematic–isotropic transition: $\tau = 1.14$ and $\tau = 1.62$, respectively, whereas the outer regions are at temperature $\tau = 0.16$. Correspondingly, the blue surfaces in *B* and *E* enclose the "hot" isotropic locally melted parts of the sample. (*Insets*) Cross-sectional views of the director configurations. The bars in these insets are color coded according to the local scalar order parameter *Q* while the guiding laser is on. (*C* and *F*) After "turning off" the guiding laser beams, the nematic configurations relax as required by the free-energy minimization, while preserving linking number or knottedness defined by the laser-guided temperature quench.

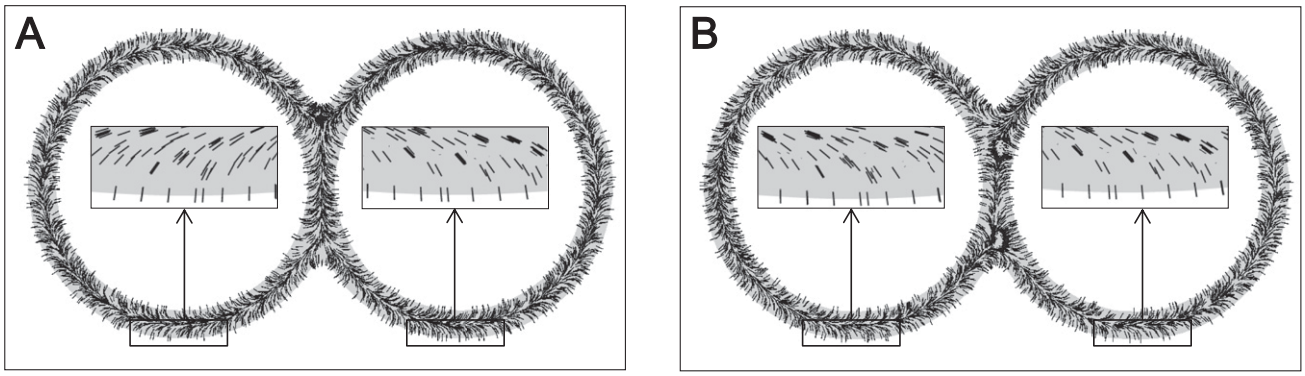

Fig. S2. Theoretical implementation of the laser-guided temperature quench used to select two different solitonic escaped configurations with different defect loops and points at the intertori regions. Here one may control the direction of the escape in each handle of a 2-tori by combing it with a linearly polarized laser light: the director escapes in the opposite (*A, Insets*) and in the same (*B, Insets*) directions defined by the orientation of linear polarization of the combing laser light. Relaxed director configurations with an elementary hedgehog charge (*A*) and with two disclination loops with the same hedgehog charge (*B*) correspond to the ones shown in Fig. 4 *A* and *B* of the main text. The loop in the lower junction of *B* carries no topological charge ($m = 0$).